MODELING AND SYNTHESIS OF THE WISTAR RAT ELECTROCARDIOGRAM

SANTIAGO FEDERICO CARACCIOLO[*,†,§],
JAVIER GUSTAVO MENDIETA[*,‡,¶] and PEDRO DAVID ARINI[*,†,‖]

[*]*Instituto de Ingeniería Biomédica, Facultad de Ingeniería*
Universidad de Buenos Aires, Av. Paseo Colón 850 piso 4
C1063ACV, Buenos Aires, Argentina

[†]*Instituto Argentino de Matemática, Alberto P. Calderón*
CONICET Saavedra 15 piso 3, C1083ACA, Buenos Aires, Argentina

[‡]*UIDET Matemática Aplicada, Facultad de Ingeniería*
Universidad Nacional de La Plata Calle 1 y 47
B1900TAG, La Plata, Buenos Aires, Argentina
[§]*scaracciolo@conicet.gov.ar*
[¶]*jgmendieta@fi.uba.ar*
[‖]*pedro.arini@conicet.gov.ar*

Received 31 March 2023
Accepted 15 June 2023
Published 3 August 2023

In this work, we present a synthesizer of electrocardiographic signals of the experimental model of the Wistar rat. Firstly, we modeled the P, R, and S waves using Gaussian functions, while for the T-wave, we used a Gumbel function. We validated the proposed model using a Wistar rat electrocardiogram database, which contains 41 animals with 62,907 beats. Model global performance was CC (correlation coefficient) $= 0.980 \pm 0.009$, and RE (relative error) $= 0.194 \pm 0.049$. We also propose a transformation that allows the aforementioned model to be built from the standard ECG parameters, such as RR interval, P wave duration, PR interval, RS interval, QT interval, and P, R, S, and T wave amplitudes. In all cases, the correlation coefficients obtained were greater than 0.966, while the mean of the absolute errors of the parameters did not exceed 6 ms and 30 μV. Also, we have developed software that integrates the proposed model and the transformation. We used a system of coupled differential equations to synthesize several beats based on one cardiac beat pattern with the possibility of entering variability in the ECG parameters and adding noise to give realism to the electrocardiographic signals. In conclusion, we developed a synthesizer of Wistar rats ECG useful for several applications, such as delineation and segmentation, training and testing of automatic algorithms to detect and monitor, as well as novel filtering methods of these types of ECG signals.

Keywords: ECGSYN; Animal Model; Heartbeat Generator.

[§]Corresponding author.

1. Introduction

Cardiovascular diseases are one of the first causes of mortality and morbidity worldwide. Animal models have contributed to the diagnosis and treatment of several cardiac diseases. Rats and mice are common species used in experimental cardiac electrophysiology. These models offer advantages relative to larger animals such as their low costs, less physiology variability, shorter evaluation times, possibility of using transgenic models, and apply many research techniques.[1]

Years of research have shown that the heart is very sensitive to toxicants via multiple ways of exposure. With the Wistar rat model, it is possible to induce pathologies or cardiovascular disorders produced by a diversity of xenobiotics and environmental stressors. It is useful to evaluate the cardiovascular effect of varenicline,[2] analyze the impact of isoprenaline and caffeine on cardiac geometry[3] or the effects of atropine and propranolol in the heart rate variability,[4] among others. Moreover, other stressors have been analyzed as air pollution, diet, and hypoxia to evaluate the initiation and evolution of cardiovascular diseases. For instance, the effects of atmospheric carbon monoxide exposure in Wistar rats,[5,6] ECG changes in obese rats[7] or the effects of systemic hypoxia with different levels of CO_2 on RR interval.[8] In addition to the studies named, the Wistar rat model is widely used to recreate acute ischemia and myocardial infarction doing coronary artery occlusions[9,10] and evaluate cardioprotective effects of drugs on ECG,[11] among others.

In most cases, data analysis carried out using Wistar rat models requires, among others, ECG recordings to evaluate the results of the experiments. For example, cardiac adverse effects in toxicology or stress studies often manifest as heart rate alterations, interval duration, and morphological changes in ECG signals. In this sense, it is essential to develop automatic delineation algorithms to obtain characteristic wave peaks and fiducial ECG points. The use of electrocardiographic signals, often long-lasting, in small rodents experiments requires that proposed automatic delineation techniques be validated. That is in ECG recordings corrupted by muscle noise, external interference, or by changes in the heart rate, postural modifications, or evaluated and validated in telemetry devices.

Many times it is convenient to use electrocardiographic recordings simulated to implement testing and evaluation of algorithms of the ECG wave delineation. Also, the designed algorithms can be implemented and validated with real ECG signals.

There are no available ECG Wistar rats public databases likewise defined assessment methodologies available to evaluate the ECG Wistar rats delineation. Moreover, most processing ECG algorithms analyze each particular experiment making performance comparisons difficult due to differences in experimental settings, such as telemetry and drugs. In this sense, it is of interest to have ECG synthesizers. Regarding ECG generators, Suppappola *et al.* have modeled the ECG as a sum of Gaussian functions.[12] This idea has been incorporated into a system of differential equations proposed by McSharry *et al.*[13] This model, called ECGSYN, was utilized to produce ECG temporal behavior, incorporating parameters such as mean and

standard deviation heart rate (HR) and LF/HF ratio.[14,15] In this sense, as far as we know, no works or reports are providing Wistar rats ECG signals generated by the ECGSYN model.

This work aims to present a procedure to synthesize electrocardiographic signals of Wistar rats using the ECGSYN model with modifications concerning the original. In this sense, we propose a novel transformation that enables the synthesis of the ECG signal from the intervals and amplitudes of the ECG, achieving a more versatile synthesis model than the one used up to now. Also, we implemented software that includes the model and the transformation in the same environment, allowing us to simulate the ECG of the Wistar rats with physiology variability and noise controlled by the operator.

2. Materials

2.1. *Database*

In this work, we used Wistar rat ECG signals acquired at the Institute of Medical Research Dr Alfredo Lanari, University of Buenos Aires, Argentina. This dataset, previously acquired to analyze ECG delineation techniques,[16] contains a group of 57 Wistar rats. The cardiac signals were digitized using ECCOSUR S.A. equipment (Buenos Aires, Argentina) at 1 kHz and 12 bits resolution (Fig. 1, Database, step 1). After anaesthesia with Ketamine (75 mg/kg) and Rompun (0.75 mg/kg xylazine) was subcutaneously administered and once the animal was stabilized, the ECG signals were continuously recorded for between 4.3 and 13.1 min (mean 5.9) in I-II, V_1, V_3, and V_6 leads.

We analyzed ECG lead II for the following reasons. Firstly, we have observed that lead II is the most used electrocardiographic lead in Wistar rat studies.[17] Secondly, this ECG lead presents P, R, S, and T waves with higher amplitude than other electrocardiographic leads. Lead II can be achieved in the Wistar rat by the placement of the negative electrode near the right shoulder and the positive electrode at the left of the xiphoid space likewise the human right arm and the left leg electrodes of the standard configuration.[1]

From the total of recordings originally acquired, we selected those presenting representative ECGs of the normal Wistar rats (Fig. 1, Database, step 2). We maintained, according to inclusion criteria those animals with positive monophasic P-wave, presence of RS-waves, good enough T-wave amplitude, and T-wave without ST-segment. In consequence, we rejected 16 Wistar rat ECGs from the original group. Finally, a group of 41 Wistar rats, 23 males (13.6 ± 8.0 weeks old and 303.8 ± 156.4 g of weight) and 18 females (18.2 ± 10.6 weeks old and 242.6 ± 99.3 g of weight) were incorporated in the present study. All these animals were in sinus rhythm at the time of ECG recordings.

Animals were cared according to Argentina's National Drug, Food and Medical Technology Administration Standards (Regulation 6344/96) and the National

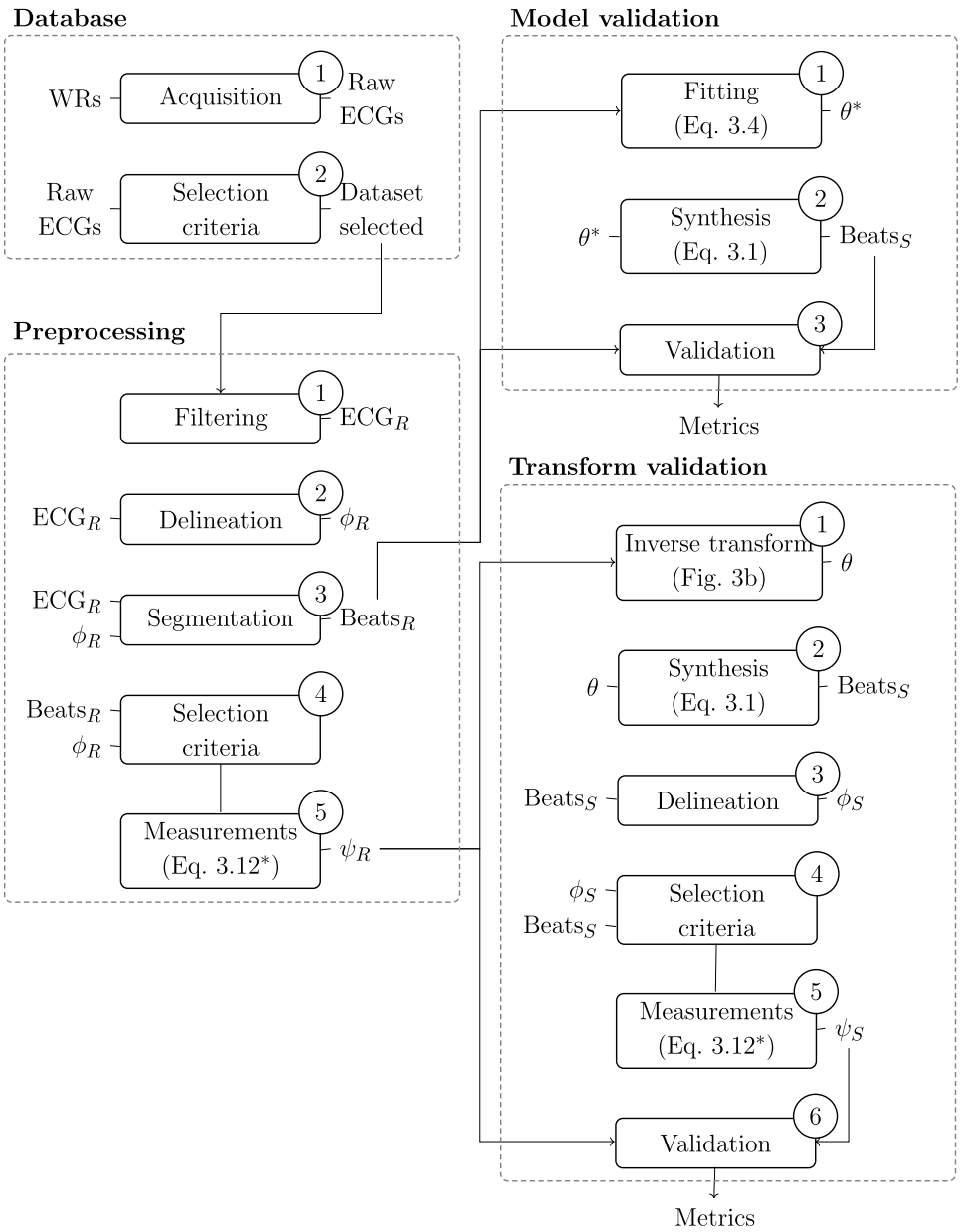

Fig. 1. Flowchart of the four stages of work: Database (**top left**), the dataset selected and used; Preprocessing (**bottom left**), the filtering and measurement of electrocardiographic parameters; Model validation (**top right**), the instance of validation of the proposed modeling and Transform validation (**bottom right**), implementing and testing of the transforms. *The last formula of the set of equations (3.12) uses the beat instead of the model.

Institute of Health Guide for the Care and Use of Laboratory Animals (NIH Pub. No. 85-23, Revised 1996).

2.2. *Characteristics of the Wistar rat ECG signals*

We have considered the most important temporal aspects of the electrocardiographic signals. The signals do not have Q-wave in the majority of ECG leads, mainly in the electrocardiographic lead II it cannot be observed.[18] We have observed a lack of an isoelectric baseline between depolarization and repolarization waves.[19] At the same time, these signals showed a short QT interval and lack of ST-segment, as we observed in our previous investigation.[16] We observed that the beginning of the T-wave was located at the same position as the end of the S-wave. However, even though Wistar rats do not have an ST segment, some perturbations that could induce changes in that segment will modify similarly the RS-waves/T-wave region of the ECG in Wistar rats.[20]

On the other hand, we have previously evaluated the power spectrum of the Wistar rat ECG.[16] That was useful to compare human and Wistar rat ECG signals. We observed that the frequency contents of ECG Wistar rats are 4–5 to 120 Hz, while humans are 0.05 to 40 Hz. The energy of the P-wave in rats goes between 20 and 60 Hz band, while the spectrum of the P-wave in humans is usually below 10–15 Hz. The T-wave in Wistar rats ranges from 5 to 80 Hz, while in humans it is below 15 Hz. The most relevant frequency content of the QRS-complex in humans is approximately between 5 and 25 Hz, while in Wistar rats ventricular depolarization energy is placed between 30 and 80 Hz.

3. Methods

3.1. *ECG pre-processing and delineation*

The Wistar rat ECG recordings, selected as described in Sec. 2.1, were filtered (Fig. 1, Preprocessing, step 1). Due to the power-line interference at 50 Hz which is located in the spectrum of the ECG Wistar rat,[16] an adaptative nonlinear notch filter was applied.[21] Baseline movement and high-frequency noise were filtered using a band-pass filter with cutoff frequencies of 2 and 300 Hz as we proposed in Ref. 16. Finally, we implemented isoelectric line correction based on the mode estimation.[22]

After the filtering process, we detected RS complexes and delineated the fiducial points of the electrocardiographic signals. To achieve this aim, we used a Wavelet-based delineator that we previously designed and validated for use in Wistar rat ECG signals[16] (Fig. 1, Preprocessing, step 2).

We obtained the localization of the onsets, peaks, and offsets of the: P-waves, RS-complexes, and T-waves. Then, we generated a Fiducial Points Table (FPT) containing the following nine positions P_{on}, P_{peak}, P_{off}, RS_{on}, R_{peak}, S_{peak}, J, T_{peak} and T_{off} for each beat of each animal. Using the FPT and computing the

mode of the RR intervals in each ECG recording, we segmented each beat (Fig. 1, Preprocessing, step 3).

Afterward, we applied the beat exclusion criteria (Fig. 1, Preprocessing, step 4) as follows: (1) each fiducial point must be in the defined beat window; (2) none of them must be NaN (not annotation); (3) those beats with a low correlation value concerning the average beat were discarded. Only those beats that present values greater than 0.90 will be accepted. Finally, we calculated RR intervals, PR intervals, P-wave durations, RS durations, and QT intervals. Also, we measured the amplitudes of P, R, S, and T waves, respectively (Fig. 1, Preprocessing, step 5). We used Python as the programming language with NumPy,[23] SciPy,[24] and SymPy[25] to compute all methods.

3.2. *Modeling*

To model the cardiac signals, we have modified the ECGSYN generator[13] according to the morphological characteristics of the Wistar rat electrocardiograms. This model generates synthetic ECG signals using a Gaussian kernel. The RS complexes and the P and T waves are defined by Gaussian functions with characteristic parameters. In our modeling, we introduced two modifications. As the Wistar rats do not have Q-wave, we eliminated that representation. Also, the Wistar rat electrocardiogram does not show the ST segment. Consequently, we replaced the Gaussian function with the Gumbel function due to the fact that it represents better the T wave morphology of Wistar rats.

The proposed model to generate a Wistar rat heartbeat is

$$f(t \,|\, \theta) = \sum_{i=\{P,R,S\}} g(t \,|\, \theta_i) + h(t \,|\, \theta_T), \tag{3.1}$$

where $\theta_i = \{a_i, \mu_i, \sigma_i\}$ represents the amplitude, location and width of the P wave and RS complex, respectively, and $\theta := \bigcup_i \theta_i$. The Gaussian function is defined as

$$g(t \,|\, \theta_i) = a_i \exp\left(-z_i^2(t)/2\right) \tag{3.2}$$

and the Gumbel function as

$$h(t \,|\, \theta_T) = a_T \exp\left(1 - z_T(t) - \exp\left(-z_T(t)\right)\right) \tag{3.3}$$

and being $z_i(t) = (t - \mu_i)/\sigma_i$. Figure 2 shows the ECG waves modeled (dotted lines) and the summation of resulting waves represented in a solid line.

3.2.1. *Model validation*

The validation is based on computing the error between the proposed model, $f(t \,|\, \theta)$, and real beats, $y(t)$, using Eq. (3.1). To do this, we perform a nonlinear fit minimizing the 2-norm estimation error, solving the problem as

$$\theta^* = \underset{\theta \in \mathbb{R}^{12}}{\operatorname{argmin}} \| f(t|\theta) - y(t) \|_2^2, \tag{3.4}$$

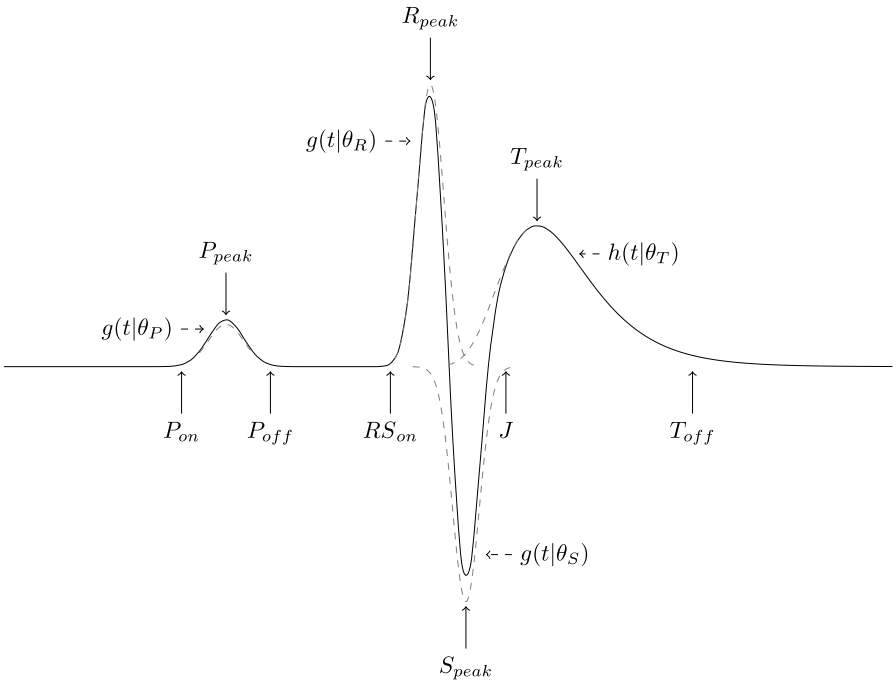

Fig. 2. An example of the Wistar rat cardiac beat synthesized using the proposed modeling. We can observe the fiducial points, indicated by an arrow, and the representation of each ECG wave in dotted lines.

where θ^* represents the optimal features of the model (Fig. 1, Model validation, step 1). We used the trust region reflective algorithm[26] implemented on *curve_fit* method of the SciPy library. We have synthesized each Wistar rat beat (Fig. 1, Model validation, step 2) using optimal parameters. Moreover, we have computed the correlation coefficient (CC) and relative error (RE) metrics (Fig. 1, Model validation, step 3),

$$\mathrm{CC} = \frac{\sum_i (x_i - \bar{x})(y_i - \bar{y})}{\sqrt{\sum_i (x_i - \bar{x})^2}\sqrt{\sum_i (y_i - \bar{y})^2}} \quad \mathrm{RE} = \frac{\|x - y\|_2}{\|y\|_2}, \tag{3.5}$$

where the bar operator is the mean value, $x := f(t \,|\, \theta^*)$ and i is the number of sample of each beat.

3.3. *Transforms*

The transform relationships between the model features, θ, the fiducial points, ϕ, and the electrocardiographic measurements, ψ, are described in this section. We defined split groups for θ and ψ, respectively. For the model features we partitioned $\theta = \theta_a \cup \theta_t$ being $\theta_a := \bigcup\{a_i\}$ the amplitude features and $\theta_t := \bigcup\{\mu_i, \sigma_i\}$ the temporal features. In addition, we divided the electrocardiographic measurements $\psi = \psi_a \cup \psi_t$, where ψ_a was related to the amplitude measurements $\{\hat{P}, \hat{R}, \hat{S}, \hat{T}\}$,

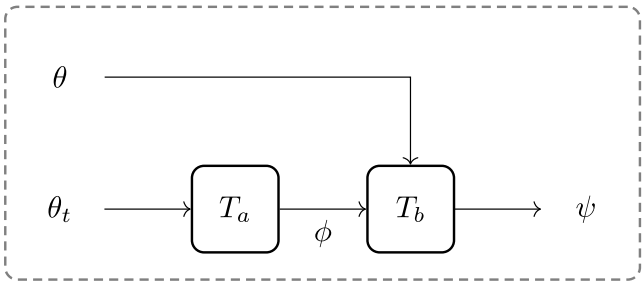

(a) Forward problem

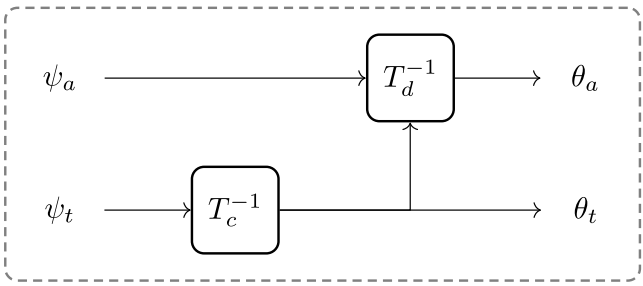

(b) Inverse problem

Fig. 3. Flowchart showing the relationship between the features of the model, the ECG fiducial points, and the electrocardiographic measurements. The top panel indicates the direct problem, i.e., obtaining the ECG parameters from the features, and the bottom panel describes the inverse problem.

and $\psi_t := \{RR, P, PR, RS, QT\}$ related to temporal measurements. Also, $\phi := \{P_{\text{on}}, P_{\text{peak}}, P_{\text{off}}, RS_{\text{on}}, R_{\text{peak}}, S_{\text{peak}}, J, T_{\text{peak}}, T_{\text{off}}\}$ defined the most relevant Wistar rat ECG fiducial points. As shown in Fig. 2, we can observe fiducial point positions to the heartbeat. Transformations between θ, ϕ and ψ are shown in Fig. 3 and each of them is developed in the following subsections.

3.3.1. *Temporal features to fiducial points* (T_a)

Using a linear transformation, we solved the forward problem denoted as $T_a : \mathbb{R}^8 \to \mathbb{R}^9$, so that

$$\begin{cases} P_{\text{on}} = \mu_P - k_P\sigma_P, \\ P_{\text{off}} = \mu_P + k_P\sigma_P, \\ RS_{\text{on}} = \mu_R - k_R\sigma_R, \\ J = \mu_S + k_S\sigma_S, \\ T_{\text{off}} = \Omega(\mu_T, \sigma_T), \\ i_{\text{peak}} = \mu_i, \quad i \in \{P, R, S, T\}, \end{cases} \tag{3.6}$$

where $k_P = 1.6$, $k_R = 3.0$, and $k_S = 2.5$ were *a priori* defined in relation to the statistical deviation and the half of each wave. We used Ω to establish the T wave end. We computed, by linear regression, the intersection of the corresponding straight line of the descending branch of the T wave contained between 80 and 40% of the T wave peak and the abscissa axis.[27]

Since the T wave was modeled as a Gumbel function, we computed the linear regression as a function of θ_T:

$$(m^*, b^*) = \underset{(m,b)\in\mathbb{R}^2}{\operatorname{argmin}} \int_{t_1}^{t_2} [h(t \,|\, \theta_T) - (mt + b)]^2 dt, \tag{3.7}$$

where $t_k > \mu_T$ and $h(t_k \,|\, \theta_T) = p_k a_T$ with $p_k = 0.8, 0.4$ for $k = 1, 2$. Once the optimization has been carried out, we compute

$$T_{\text{off}} = -b^*/m^*. \tag{3.8}$$

To optimize Eq. (3.7), we applied a variable change as follows: $z = (t - \mu_T)/\sigma_T$, then we solved the equivalent problem as

$$(\mathbf{m}^*, \mathbf{b}^*) = \underset{(\mathbf{m},\mathbf{b})\in\mathbb{R}^2}{\operatorname{argmin}} \int_{z_1}^{z_2} [h(z) - (\mathbf{m}z + \mathbf{b})]^2 dz. \tag{3.9}$$

We obtained the limits of the integral solving the problem $z_k \in \mathbb{R}_{>0} : p_k = \exp(1 - z_k - \exp(-z_k))$ whose values were obtained explicitly as $z_k = -\ln(-\mathcal{W}(-p_k/e))$, where $\mathcal{W}$ is the Lambert function. The relationship between the variables of (3.7) and (3.9) is given by

$$\mathbf{m} = \frac{m\sigma_T}{a_T}, \quad \mathbf{b} = \frac{m\mu_T + b}{a_T}, \tag{3.10}$$

therefore, obtaining m and b from (3.10) and substituting the optima in (3.8) we get $T_{\text{off}} = \mu_T - k_T\sigma_T$ with $k_T = -\mathbf{b}^*/\mathbf{m}^*$ whose value is obtained by solving (3.9) by finding extreme points with partial derivatives, and the result is

$$k_T = \frac{q_{0,1}(q_{2,0}q_{0,0} - q_{1,0}^2) - q_{1,0}(q_{1,1}q_{0,0} - q_{0,1}q_{1,0})}{q_{0,0}(q_{1,1}q_{0,0} - q_{0,1}q_{1,0})} \approx -2.6891 \tag{3.11}$$

being $q_{i,j} = \int_{z_1}^{z_2} z^i h(z)^j dz$. With the obtained result we notice that T_a transform of Eq. (3.6) is linear and can be expressed in matrix form.

3.3.2. *Fiducial points to electrocardiographic measurements* (T_b)

That is the transformation commonly used in electrocardiography. It is nonlinear due to the use of the features θ that represent the model $f(t \,|\, \theta)$ of the cardiac beats, as we illustrated in Fig. 3. It is defined as $T_b : \mathbb{R}^9 \to \mathbb{R}^9$,

so that

$$\begin{cases} RR = 2R_{\text{peak}}, \\ P = P_{\text{off}} - P_{\text{on}}, \\ PR = RS_{\text{on}} - P_{\text{on}}, \\ RS = J - RS_{\text{on}}, \\ QT = T_{\text{off}} - RS_{\text{on}}, \\ \hat{k} = f(k_{\text{peak}} \,|\, \theta), \quad k \in \{P, R, S, T\}. \end{cases} \tag{3.12}$$

3.3.3. *Temporal features to temporal measurements* (T_c)

Obtaining the temporal features of the model from the measurements is an ill-posed inverse problem which is dealt with applying constraints to the problem.

Firstly, we constructed $T_c : \mathbb{R}^8 \to \mathbb{R}^5$ lineal, from the replacement of (3.6) in the linear region of (3.12) (excluding the last four equations),

$$\begin{cases} RR = 2\mu_R, \\ P = 2k_P\sigma_P, \\ PR = (\mu_R - k_R\sigma_R) - (\mu_P - k_P\sigma_P), \\ RS = (\mu_S + k_S\sigma_S) - (\mu_R - k_R\sigma_R), \\ QT = (\mu_T - k_T\sigma_T) - (\mu_R - k_R\sigma_R). \end{cases} \tag{3.13}$$

Afterwards, we added three hypotheses to constrain the problem and obtained a unique inverse T_c^{-1}:

$$\sigma_R = k_w\sigma_S \quad \text{Width ratio between R and S waves,} \tag{3.14}$$

$$\mu_S = \mu_R + k_d\sigma_R \quad \text{Distance between R and S peaks,} \tag{3.15}$$

$$t_J = \mu_S + k_S\sigma_S \quad J \text{ is the Gumbel inflexion point,} \tag{3.16}$$

where $t_J = \mu_T + \ln(\frac{3-\sqrt{5}}{2})\sigma_T$. Equation (3.16) is obtained from the hypothesis that J point coincides with the inflexion point of the Gumbel function, that is, $t_J < \mu_T : \frac{d^2}{dt^2}h(t_J \,|\, \theta_T) = 0$. The values of k_w and k_d were evaluated as 1.0 and 2.0, respectively.

3.3.4. *Amplitude features to amplitude measurements* (T_d)

Once θ_t through T_c^{-1}, we use the last four equations of (3.12) to define the nonlinear transformation, $T_d : \mathbb{R}^4 \to \mathbb{R}^4$ so that $\hat{k} = f(\mu_k \,|\, \theta_t)$, $k \in \{P, R, S, T\}$. Whose inverse solution is obtained with the nonlinear solver called *broyden1* in SciPy library and using $\theta_a^0 := \psi_a$ as initial values.

3.3.5. *Transform validation*

We obtained the features of the model by applying the transform to the entire temporal and amplitude measurements (Fig. 1, Transform validation, step 1). After that, we synthesized beats (Fig. 1, Transform validation, step 2) which were later delineated (Fig. 1, Transform validation, step 3). We applied the selection criteria described in Sec. 2.1 (Fig. 1, Preprocessing, step 4), but in that case over synthesized ECG signals. Finally, we used the fiducial points to calculate ECG measurements coming from the synthesized signals (Fig. 1, Preprocessing, step 5).

The validation arises from the comparison between real measurements belonging to the database versus synthesized signals using the transform proposed (Fig. 1, Preprocessing, step 6). We show that comparison by Pearson and Bland & Altman graphs in Figs. 5(a) and 5(b).

3.4. *Wistar rats ECG synthetizer*

We designed real-time software to produce a cardiac beat by feeding the cascade blocks, inverse transform and model, with the ECG measurements, ψ, as we can see in Fig. 4(a). Figure 4(b). represents the ECG synthesis phase which provides the possibility to introduce variability based on the features obtained in the design

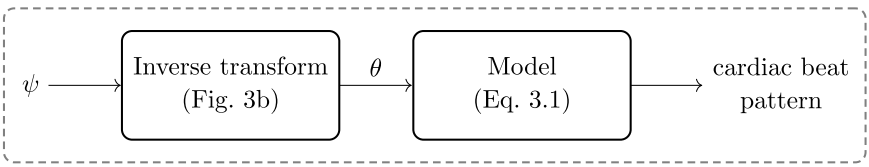

(a) Beat design phase

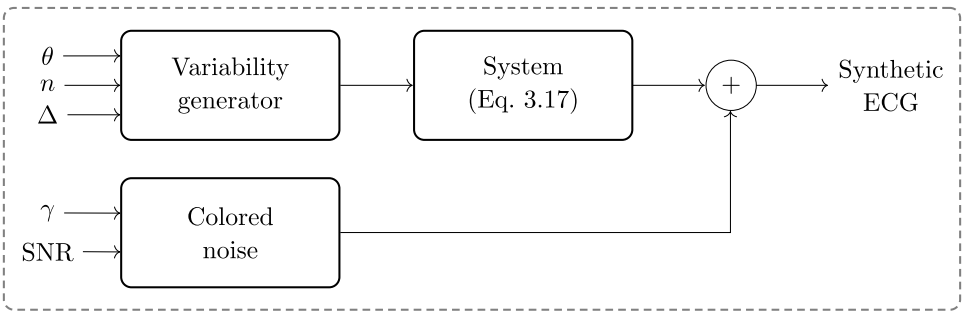

(b) ECG synthesizer phase

Fig. 4. Flowcharts showing the two main phases of the ECG synthesis software. (a) Heartbeat pattern generator in real-time. (b) ECG synthesis phase. n: number of generated beats; Δ: percentage of parameters variabilities; γ: exponent that defines the noise color; SNR: signal-to-noise ratio.

stage. The variability generator builds features with Gaussian distribution using θ as the mean value, Δ as a proportion to compute the standard deviation and n as the number of beats to synthesize. The system block computes the ECGSYN differential equations,[13]

$$\begin{cases} \dot{x} = \alpha x - \omega y, \\ \dot{y} = \alpha y + \omega x, \\ \dot{z} = \dot{f}(\beta \,|\, \theta_\omega), \end{cases} \tag{3.17}$$

where $\alpha = 1 - \sqrt{x^2 + y^2}$, $\beta = \arctan 2(y, x)$ and $\omega = 2\pi/RR$. The first two equations of (3.17) represent a particle rotating in the XY plane with unit radius at a speed of RR seconds per full turn. The model features are scaled such that $\theta_\omega := \theta_a \cup w\theta_t$ which allows transforming from the time variable to angle $\beta = \omega t \mod 2\pi$.

The bottom branch of Fig. 4(b) shows the sum of noise, at different SNRs and colors determined by the exponent in $(1/f)^\gamma$, that generates noisy ECGs with a realistic morphology.

4. Results

We computed the CC and RE between all real beats and their respective beats adjusted to show the level of fit of Eq. (3.1) for the Wistar rats complete database. The quartiles obtained for CC metric are $Q1 = 0.974$, $Q2 = 0.981$, and $Q3 = 0.986$ and for the RE metric they are $Q1 = 0.164$, $Q2 = 0.195$, and $Q3 = 0.227$. We have applied these metrics for a total of 62,907 real ECG beats obtained from 41 Wistar rats. Likewise, we evaluated the transform validation as we show in Figs. 5(a) and 5(b). We made Pearson and Bland & Altman plots for temporal and amplitude measurements between real and synthesized beats. We observed a good prediction for all parameters since in all cases, $\rho \approx 1$. Due to the fact that ρ does not detect differences in scale, we provide the slope m to show the trend of the points cloud.

Additionally, the Bland & Altman plot allows us to observe the mean and standard deviation of the parameter differences between real and synthesized beats. The worst case was the duration of the RS interval, the mean of difference being 2.1 ms and its physiological values being from 18 to 26 ms.

To illustrate the model and the transformation, we developed software that synthesizes the ECG signals using the modified ECGSYN, as we proposed in this work. The software requires the input of the ECG parameters, then the transformation is executed in real-time, and with the obtained features, a beat with the desired characteristics is computed. Subsequently, with the system of equations (3.17) the beats are synthesized. Figure 6 shows nine synthetic Wistar rat beats using the

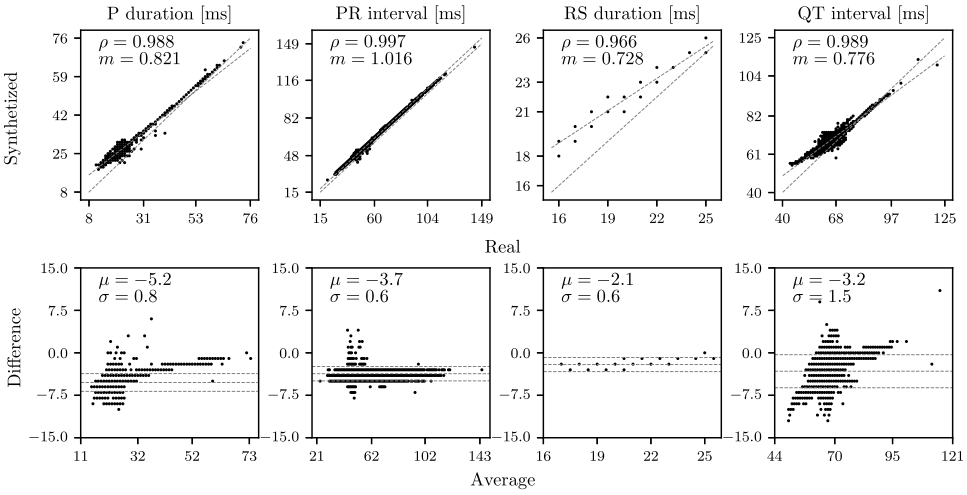

(a)

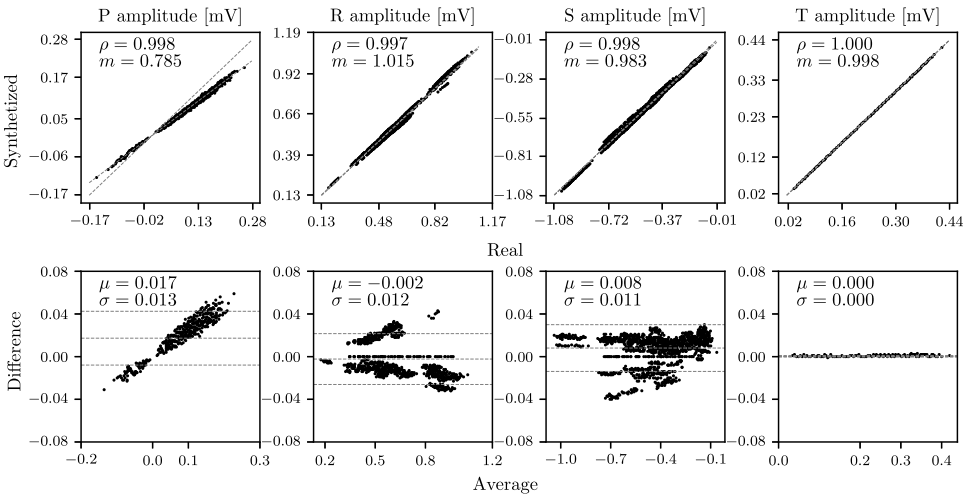

(b)

Fig. 5. The results of the Transform Validation (Sec. 3.3.5). Panel (a) is for durations and (b) for amplitudes of ECG parameters. For each panel, the Pearson plot is on the top and Bland & Altman plot is on the bottom. Each plot contains 59,183 validation values obtained from 41 Wistar rats. The dotted lines on the Pearson plot represent the ideal fit line, while on the Bland & Altman plot are $\mu \pm 1.96\sigma$.

following input parameters: $RR = 140\,\text{ms}$, $P = 10\,\text{ms}$, $PR = 40\,\text{ms}$, $RS = 15\,\text{ms}$, $QT = 60\,\text{ms}$, $P_{\text{peak}} = 110\,\mu\text{V}$, $R_{\text{peak}} = 500\,\mu\text{V}$, $S_{\text{peak}} = -300\,\mu\text{V}$, $T_{\text{peak}} = 300\,\mu\text{V}$. Also, we have incorporated ECG parameters variations of $\Delta RR = 0\%$, $\Delta P = 5\%$, $\Delta PR = 5\%$, $\Delta RS = 5\%$, $\Delta QT = 5\%$, $\Delta P_{\text{peak}} = 50\%$, $\Delta R_{\text{peak}} = 15\%$,

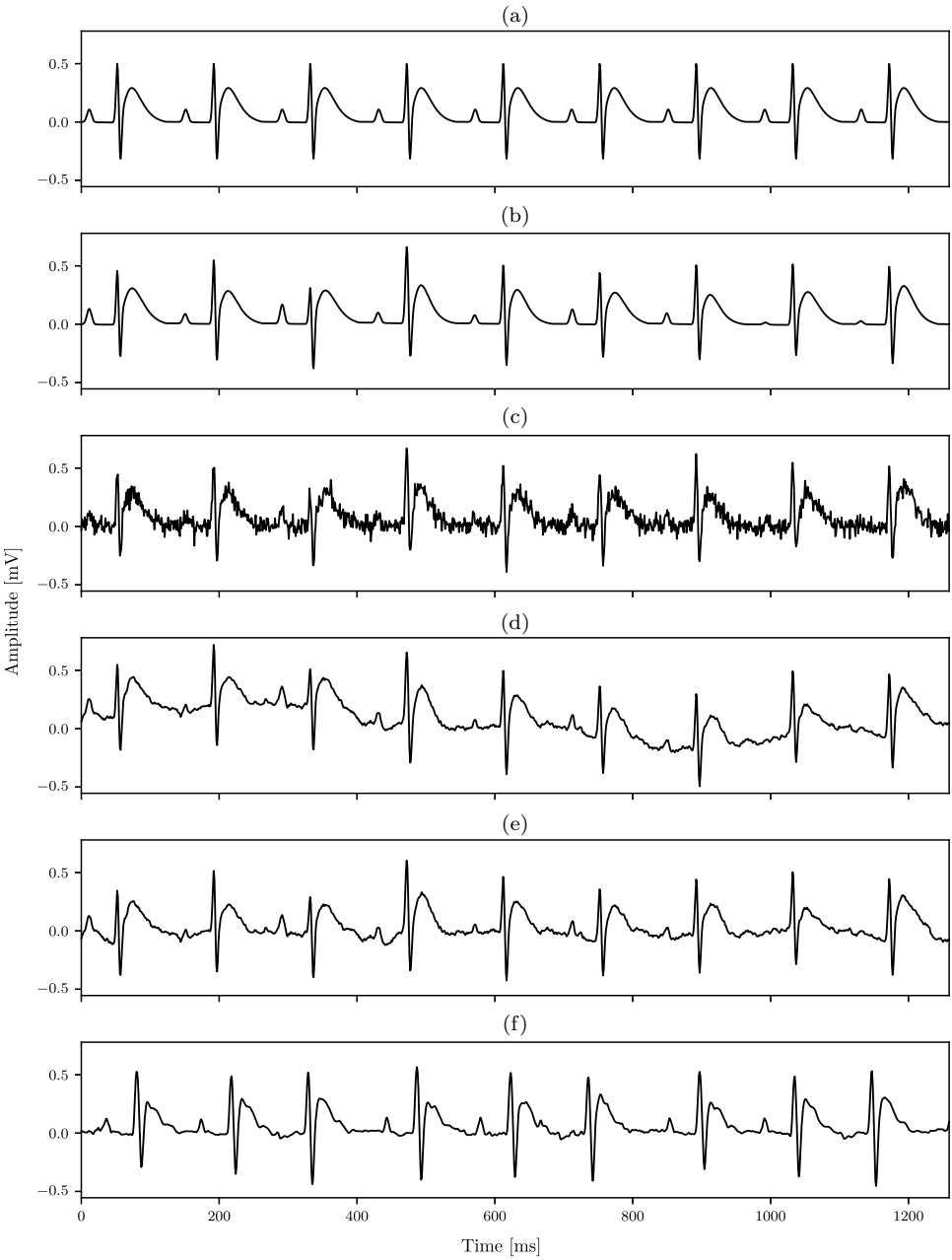

Fig. 6. Example of synthetic Wistar rat ECGs, from (a) to (e). (a) Cardiac beats pattern. (b) Cardiac beats with parameter variations. (c) Cardiac beats with the addition of 10 dB white noise. (d) Cardiac beats with the addition of 4 dB Brownian noise. (e) The same ECG that in (d) but with baseline removal. (f) Real Wistar rat ECG obtained from the database.

$\Delta S_{\text{peak}} = 15\%$, $\Delta T_{\text{peak}} = 15\%$. Finally, we have incorporated white noise with 10 dB and Brownian noise with 4 dB.

5. Discussion

The Wistar rat experimental laboratory model provides advantages concerning larger animals as their low cost, less physiology variability, shorter evaluation times, the possibility of using transgenic models, and the option of applying many research techniques.

This experimental model recreates, in the laboratory, acute ischemia, myocardial infarction, cardioprotective effects of drugs, pathologies produced by a diversity of xenobiotics, and analyzes general anaesthesia, among others. In the present work and concerning everything explained above, we have proposed implementing a framework capable of modeling and synthesizing Wistar rat cardiac beats.

We adapted the original model[13] by removing the Q wave and adding the Gumbel function to more faithfully represent the T wave of the Wistar rat. The proposed model has been tested against a database of Wistar rats ECG signals and the metrics show a good fit for the model. As far as we know, this is the first work that presents a mathematical model to synthesize electrocardiographic signals of Wistar rats.

Also, we have extended through the transformation of Fig. 3(b). the ECGSYN with the possibility of synthesizing ECG Wistar rats from ECG intervals (RR, P, PR, RS, and QT) and amplitudes (P, R, S, and T). Without this transformation, the model is fed with mathematical features with poorly physiological meaning. We emphasize that the described information is not available for the operator (namely researchers), preventing the exploitation of the potential that the ECGSYN synthesis model possesses in itself. Therefore our proposal achieves a more realistic and versatile synthesizer *in-silico* model.

To obtain a good performance of the transform proposed, we applied several hypotheses. We considered the agreement between the J point and the inflexion point of the Gumbel function (Eq. (3.16)), the distance between R and S peaks (Eq. (3.15)) and the relationship between them (Eq. (3.14)) and the P wave symmetry (Eq. (3.13)), among others. These considerations are simplifications that introduce errors in the estimates. However, we highlight that the transformation is simple but enough to capture the desired morphology with relatively low errors (Fig. 5).

In another sense, the RS parameter presents poor performance, due to the fact that its value strongly depends on the interaction of the R, S, and T waves, as can be seen in Fig. 2.

Finally, we highlight that the simplicity of the transformation allowed us the design a Wistar rat heartbeat in real-time using the developed software.

6. Study Limitations

We observed that the results of transform validation were slightly affected by the ECG delineator performance. The P wave is the most difficult wave to delineate

because of its low SNR. Also, we take into account that the model metrics represent global values and there may be areas in the cardiac beat that are better adjusted than others. The most revealing case is the PR segment. The delineation of P_{off} is also challenging because of the unevenness of the segment PR. The PR segment is usually below the isoelectric level in the Wistar rat ECG. This phenomenon is not represented correctly by Gaussian functions that always start and end at the isoelectric level.

7. Conclusions

We have developed a procedure to synthesize electrocardiographic signals of Wistar rats using a modified ECGSYN and a novel transformation that relates ECG parameters and the features of the model.

We synthesized the ECG signal feeding the synthesizer with the RR, P, PR, RS, and QT intervals and their P, R, S, and T amplitudes of the ECG waves. Also, we have implemented software that includes the proposed model and the transformation in the same environment, allowing us to simulate the ECG of Wistar rats with physiology variability and noise determined by the operator.

In conclusion, we produce a synthesizer of Wistar Rats ECG useful for several applications, such as delineation and segmentation, training and testing of automatic algorithms to detect and monitor, as well as novel filtering methods of these types of ECG signals.

Acknowledgments

This work was supported by grants from Consejo Nacional de Investigaciones Científicas y Técnicas (CONICET), Universidad de Buenos Aires (UBA) and Agencia Nacional de Promoción Científica y Tecnológica (MINCyT), all of them from Argentina.

P.D. Arini and S.F. Caracciolo's work was supported by grants CONICET PIP 112-20130100552CO and MINCyT PICT 2145-2016.

References

1. Farraj AK, Hazari MS, Cascio WE, The utility of the small rodent electrocardiogram in toxicology, *Toxicol Sci* **121**(1):11–30, 2011.
2. Selcuk EB, Sungu M, Parlakpinar H, Ermis N, Taslidere E, Vardi N, Yalinsoy M, Sagir M, Polat A, Karatas M, Kayhan-Tetik B, Evaluation of the cardiovascular effects of varenicline in rats, *Drug Des Dev Ther* **9**:5705–5717, 2015.
3. Ahmad A, Sattar MZA, Rathore HA, Khan SA, Lazhari MA, Hashmi F, Abdullah NA, Johns EJ, Impact of isoprenaline and caffeine on development of left ventricular hypertrophy and renal hemodynamic in Wistar Kyoto rats, *Acta Pol Pharm - Drug Res* **72**(5):1015–1026, 2015.
4. Sayin H, Chapuis B, Chevalier P, Barres C, Julien C, Assessment of cardiac autonomic tone in conscious rats, *Auton Neurosci* **194**:26–31, 2016.

5. Andre L, Boissière J, Reboul C, Perrier R, Zalvidea S, Meyer G, Thireau J, Tanguy S, Bideaux P, Hayot M, Boucher F, Obert P, Cazorla O, Richard S, Carbon monoxide pollution promotes cardiac remodeling and ventricular arrhythmia in healthy rats, *Am J Respir Crit Care Med* **181**(6):587–595, 2010.
6. Meyer G, Tanguy S, Obert P, Reboul C, Carbon monoxide urban air pollution: Cardiac effects, in *Advanced Topics in Environmental Health and Air Pollution Case Studies*. IntechOpen, August 2011.
7. Mutiso S, Rono D, Bukachi F, Relationship between anthropometric measures and early electrocardiographic changes in obese rats, *BMC Res Notes* **7**(1):931, 2014.
8. Murasato Y, Hirakawa H, Harada Y, Nakamura T, Hayashida Y, Effects of systemic hypoxia on R–R interval and blood pressure variabilities in conscious rats, *Am J Physiol* **275**(3 Pt 2):H797–804, 1998.
9. Miranda A, Costa-E-Sousa RH, Werneck-De-Castro JPS, Mattos EC, Olivares EL, Ribeiro VP, Silva MG, Goldenberg RCS, Campos-De-Carvalho AC, Time course of echocardiographic and electrocardiographic parameters in myocardial infarct in rats, *An Acad Bras Cienc* **79**(4):639–648, 2007.
10. Pimentel EB, de Moraes AC, Forechi L, Machado RC, Baldo MP, Mill JG, Kinetics of the electrocardiographic changes after permanent coronary occlusion in rats: Relationship with infarct size, *Pathophysiology* **19**(4):277–281, 2012.
11. Sheibani M, Nezamoleslami S, Faghir-Ghanesefat H, Emami AH, Dehpour AR, Cardioprotective effects of dapsone against doxorubicin-induced cardiotoxicity in rats, *Cancer Chemother Pharmacol* **85**(3):563–571, 2020.
12. Suppappola S, Sun Y, Chiaramida S, Gaussian pulse decomposition: An intuitive model of electrocardiogram waveforms, *Biomed Eng* **25**:252–260, 1997.
13. McSharry PE, Clifford GD, Tarassenko L, Smith LA, A dynamical model for generating synthetic electrocardiogram signals, *IEEE Trans Biomed Eng* **50**(3):289–294, 2003.
14. Clifford GD, McSharry PE, A nonlinear artificial model for generating realistic correlated ECG, BP and respiration, *Int EURASIP Conf 17th*, pp. 358–360, 2004.
15. Clifford GD, Shoeb A, McSharry PE, Janz BA, Model-based filtering, compression and classification of the ECG, *Int J Bioelectromagn* **7**(1):158–161, 2005.
16. Arini PD, Liberczuk S, Mendieta JG, María MS, Bertrán GC, Electrocardiogram delineation in a Wistar rat experimental model, in *Computational and Mathematical Methods in Medicine*, February 2018.
17. Botelho AFM, Joviano-Santos JV, Santos-Miranda A, Menezes-Filho JER, Soto-Blanco B, Cruz JS, Guatimosim C, Melo MM, Non-invasive ECG recording and QT interval correction assessment in anesthetized rats and mice, *Pesqui Vet Bras* **39**:409–415, 2019.
18. Konopelski P, Ufnal M, Electrocardiography in rats: A comparison to human, *Physiol Res* **65**(5):717–725, 2016.
19. Fraser RS, Harley C, Wiley T, Electrocardiogram in the normal rat, *J Appl Physiol* **23**(3):401–402, 1967.
20. Detweiler DK, Electrocardiographic monitoring in toxicological studies: Principles and interpretations, in Spitzer JJ (ed.), *Myocardial Injury*, Advances in Experimental Medicine and Biology, Springer US, Boston, MA, pp. 579–607, 1983.
21. Ahlstrom ML, Tompkins WJ, Digital filters for real-time ECG signal processing using microprocessors, *IEEE Trans Biomed Eng* **32**(9):708–713, 1985.
22. Pilia N, Nagel C, Lenis G, Becker S, Dössel O, Loewe A, ECGdeli — An open source ECG delineation toolbox for MATLAB, *SoftwareX* **13**, 2021.

23. Harris CR, Millman KJ, van der Walt SJ, Gommers R, Virtanen P, Cournapeau D, Wieser E, Taylor J, Berg S, Smith NJ, Kern R, Picus M, Hoyer S, van Kerkwijk MH, Brett M, Haldane A, Fernández del Río J, Wiebe M, Peterson P, Gérard-Marchant P, Sheppard K, Reddy T, Weckesser W, Abbasi H, Gohlke C, Oliphant TE, Array programming with NumPy, *Nature* **585**(7825):357–362, 2020.
24. Virtanen P, Gommers R, Oliphant TE, Haberland M, Reddy T, Cournapeau D, Burovski E, Peterson P, Weckesser W, Bright J, van der Walt SJ, Brett M, Wilson J, Millman KJ, Mayorov N, Nelson ARJ, Jones E, Kern R, Larson E, Carey CJ, Polat I, Feng Y, Moore EW, VanderPlas J, Laxalde D, Perktold J, Cimrman R, Henriksen I, Quintero EA, Harris CR, Archibald AM, Ribeiro AH, Pedregosa F, van Mulbregt P, SciPy 1.0: Fundamental algorithms for scientific computing in Python, *Nat Methods* **17**(3):261–272, 2020.
25. Meurer A, Smith CP, Paprocki M, Certík O, Kirpichev SB, Rocklin M, Kumar A, Ivanov S, Moore JK, Singh S, Rathnayake T, Vig S, Granger BE, Muller RP, Bonazzi F, Gupta H, Vats S, Johansson F, Pedregosa F, Curry MJ, Terrel AR, Roučka Š, Saboo A, Fernando I, Kulal S, Cimrman R, Scopatz A, SymPy: Symbolic computing in Python, *PeerJ Comput Sci* **3**:e103, 2017.
26. Branch MA, Coleman TF, Li Y, A subspace, interior, and conjugate gradient method for large-scale bound-constrained minimization problems, *SIAM J Sci Comput* **21**(1):1–23, 1999.
27. McLaughlin NB, Campbell RWF, Murray A, Effects of filtering and algorithm parameters on automatic QT measurement techniques, *Computers in Cardiology 1994*, pp. 221–224, 1994.